Bioorganic Chemistry **27,** 89–97 (2000)
doi:10.1006/bioo.2000.1163, available online at http://www.idealibrary.com on IDEAL®

Rate Limitations in the Lumazine Synthase Mechanism

Ya-Jun Zheng,* Paul V. Viitanen,† and Douglas B. Jordan‡,[1]

**E. I. DuPont Agricultural Products, Stine-Haskell Research Center, 1094 Elkton Road, P.O. Box 30, Newark, Delaware 19714-0030; †E. I. DuPont Central Research and Development, Experimental Station, Wilmington, Delaware 19880-0402; and ‡DuPont Pharmaceutical Company, Stine-Haskell Research Center, 1094 Elkton Road, P.O. Box 30, Newark, Delaware 19714-0030*

Received November 16, 1999

Lumazine synthase has a slow rate of catalysis: steady-state k_{cat} values for the *Escherichia coli*, *Magnaporthe grisea*, and spinach enzymes are 0.024, 0.052, and 0.023 s^{-1}, respectively, at pH 7.5 and 25°C. Following the formation of an imine connecting the two substrates 3,4-dihydroxy-2-butanone 4-phosphate and 4-ribitylamino-5-amino-2,6-dihydroxypyrimidine, there is a chemically difficult isomerization. Calculated estimates of the free energy barrier for the isomerization are equal to or greater than 15 kcal/mol at 25°C. Free energies calculated from the steady-state k_{cat} values at 25°C for the *E. coli*, *M. grisea*, and spinach enzymes are 19.7, 19.2, and 19.7 kcal/mol, respectively. The single-turnover rate (pre-steady state) at pH 7.5 and 25°C for the *M. grisea* enzyme is 140-fold greater than the steady-state rate and it has a free energy barrier of 16.3 kcal/mol. In the pre-steady state the *M. grisea* enzyme has a pK_a of 5.8, plausibly reporting the proposed general base of catalysis (His127). The *M. grisea* enzyme has an off rate of 0.37 s^{-1} for its product, 6,7-dimethyl-8-ribityllumazine, approximately 7-fold higher than k_{cat} and 20-fold lower than the single-turnover rate. The off rate for the product orthophosphate is about 1 s^{-1}. Thus, for the *M. grisea* enzyme at pH 7.5 and 25°C, product dissociation is significantly rate limiting to the steady-state rate of catalysis, whereas the isomerization step limits the single turnover rate. The spinach and *E. coli* enzymes display a significant lag in pre-steady state, suggesting that substrate association is significantly rate limiting for these catalysts. Temperature studies on the enzyme-catalyzed rates for the three enzymes indicate a dominating enthalpic term.

INTRODUCTION

Lumazine synthase (LS) catalyzes the penultimate step of riboflavin biosynthesis (*1–4*). A molecule of 3,4-dihydroxy-2-butanone 4-phosphate (DHBP) and one of 4-ribitylamino-5-amino-2,6-dihydroxypyrimidine (RAADP) are joined to form 6,7-dimethyl-8-(1′-D-ribityl)lumazine (DMRL) with the elimination of orthophosphate and two waters. Subsequently, riboflavin synthase (RS) catalyzes the dismutation of two molecules of DMRL to yield an equivalent of riboflavin and RAADP. LS can exist as a 60-mer in the form of an icosahedral capsid with or without a trimer of RS

[1] To whom correspondence and reprint requests should be addressed. Fax: (302) 366-5738. E-mail: doug.b.jordan@dupontpharma.com.

0045-2068/00 $35.00

localized within (*5–11*) or as a pentamer lacking an association with RS (8,11,12), depending on its biological source and its condition. Association of the two terminal enzymes (LS and RS) of the pathway has been described as an instrument towards increasing catalytic efficiency (at low substrate concentrations) through a substrate-channeling mechanism (13). According to X-ray crystallographic studies, the quaternary structure of LS is determined by contacts of amino acid side chains that allow or disallow associations of pentamers (the minimal functional unit because of the organization of five active sites per pentamer) in forming a dodecrahedron of the pentamers (8,11,12). On the basis of its lack of functional counterparts in off-target organisms (e.g., humans and other animals) LS is a target for the design of inhibitors in antimicrobial programs (*14–16*).

In the crystal structures of LS, both the phosphate and the ribitylpyrimidine binding sites have been identified (*6,7,11*), allowing for a detailed mechanism to be proposed (*7,8*). Inspection of the proposed reaction path (Fig. 1) leads to the idea that the most difficult chemical step is in the isomerization of the double bond in the conversion of **3** to **4.** Unlike isomerization reactions catalyzed by numerous enzymes that employ active-site residues as general acids and bases, the isomerization of **3** to **4** is aprotic thus making it difficult for the enzyme to influence the rate. Thermal isomerization around a carbon–carbon double bond normally includes a large energy barrier; for instance, the barrier for a CHD=CHD isomerization is 65 kcal/mol (17). The activation energy for isomerization around a carbon–nitrogen double bond (as in transforming **3** to **4**) is expected to be smaller, but not insignificant. Indeed, the reported steady-state k_{cat} values for LS indicate a rather slow rate for catalysis (*3,4,10,11*). Here we examine the magnitude of the energy barrier for the isomerization step of the LS-catalyzed reaction (**3** to **4**) using a theoretical approach and compare the results to the rates of catalysis (steady-state and pre-steady state) observed for three LSs obtained from phylogenetically diverse sources.

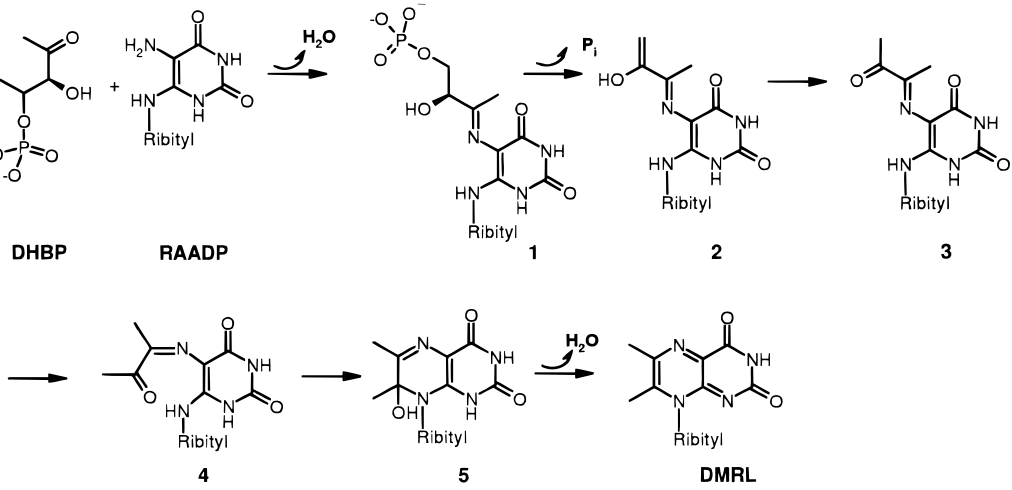

FIG. 1. The reaction path for the LS catalyzed reaction as modified from references 7 and 8.

MATERIALS AND METHODS

General. LS from *M. grisea* (11) and spinach (10) were cloned, expressed in *E. coli*, and purified as described. The *E. coli* LS was cloned and expressed in a similar fashion as reported (8); purification procedures were quite similar to those used for the *M. grisea* and spinach enzymes (10,11). Active site concentrations (one per protomer) were estimated from the 280-nm absorbencies of the proteins using extinction coefficients calculated through the Peptidesort program of the Genetics Computer Group (Wisconsin Package, Version 9, Genetics Computer Group, Madison, WI). LS substrates DHBP and RAADP were prepared as before (10). The product 6,7-dimethyl-8-ribityllumazine (DMRL) was synthesized from RAADP and 2,3-butadione (18). 2-amino-6-mercapto-7-methylpurine ribonucleoside and purine-nucleoside phosphorylase were from Molecular Probes (Eugene, Oregon). Unless indicated otherwise, linear and nonlinear least squares fittings were through the computer program RS1 (BBN Research Systems; Cambridge, MA).

Calculations. The geometry of each species was fully optimized unless otherwise indicated. For the ab initio calculations, the G2 theory (*19–21*) was used; for the semiempirical calculations, the AM1 method was employed (*22*).

Reactions. Steady-state parameters were determined at 25°C in 50 mM Tris–HCl, pH 7.5, and 1.0 mM dithiothreotol. The 1-ml reactions (60–300 s) included 1.0 mM RAADP when the rate limitation of varied DHBP concentrations was measured; the reactions included 1.0 mM DHBP when the rate limitation of varied RAADP concentrations was measured. Reactions were initiated with enzyme and the rates were recorded continuously on a HP 8542A spectrophotometer (Hewlett-Packard) by using a spectrophotometric method (10) that measures DMRL formation at 408 nm. Data were fitted to Eq. [1] for the determination of kinetic constants. k_{cat} is maximum velocity, K is the Michaelis constant, A is the varied substrate concentration, and v is the observed velocity.

$$v = \frac{k_{cat}}{1 + K/A} \qquad [1]$$

Steady-state measurements of k_{cat} at varied temperatures were conducted on a thermostated stopped-flow instrument (Applied Photophysics; Leatherhead, UK). Reactions (60 s) at varied temperatures were monitored for absorbency increases at 408 nm to detect product DMRL. The left syringe contained 1.0 mM DHBP in 100 mM sodium phosphate, pH 7.0; the right syringe contained 0.05 mM LS (*E. coli, M. grisea* or spinach LS), 1.5 mM RAADP, and 2.0 mM dithiothreitol in 100 mM sodium phosphate. The left and right syringes were mixed using equal volumes of each; the instrument dead time was estimated as 1.6 ms. Rate data were fitted to the instruments software for a burst followed by a steady state in determining the steady-state rate for the *M. grisea* enzyme and to a line for the *E. coli* and spinach enzymes.

Pre-steady state measurements at varied temperatures (25−40.5°C) and pH 7.5 were conducted on the thermostated stopped-flow instrument. The left syringe contained 0.15 mM RAADP, 1.5 mM DHBP, 1.0 mM dithiothreitol, and 200 mM Tris–HCl at pH 7.5. The right syringe contained 0.5 mM *E. coli, M. grisea*, or spinach LS. Absorbency increases were monitored at 408 nm to detect product DMRL. The single-turnover data for the *M. grisea* enzyme were fitted to a single exponential using the instruments software.

Pre-steady state measurements at varied pH (5.73 to 9.44) and 25°C were conducted on the thermostated stopped-flow instrument. The left syringe contained 0.15 mM RAADP, 1.5 mM DHBP, 1.0 mM dithiothreitol, and 200 mM Bis-Tris-Propane at varied pH. The right syringe contained 0.5 mM *M. grisea* LS in 50 mM Tris–HCl at pH 7.5. Absorbency increases were monitored at 408 nm to detect product DMRL. The single-turnover rates were fitted to a single exponential using the instruments software. Determined rates at varying pH values were fitted to Eq. [2], which describes the titration of two ionizable groups (one per side) causing a decrease on the basic side and the acidic side. *p* Represents the measured parameter, *P* is the pH independent value for the parameter, [*H*+] is the proton concentration, and K_a and K_b are the dissociation constants for the groups affecting catalysis.

$$p = \frac{P}{1 + K_b/[H+] + [H+]/K_a} \qquad [2]$$

Pre-steady state measurements at 25°C and pH 7.5 to detect orthophosphate production and release from the *M. grisea* LS were conducted on the thermostated stopped-flow instrument using purine-nucleoside phosphorylase as the coupling enzyme (23). The left syringe contained 30 units/ml purine nucleoside phosphorylase, 1.0 mM DHBP, 1.0 mM 2-amino-6-mercapto-7-methylpurine ribonucleoside, and 50 mM Tris–HCl at pH 7.5. The right syringe contained 1.5 mM RAADP, 0.1 mM *M. grisea* LS, 1.0 mM dithiothreitol, and 50 mM Tris–HCl at pH 7.5. The reactions were monitored for absorbency at 360 nm. Rates were fitted to a burst followed by a steady state using the instruments software.

Binding rates of DMRL to the *M. grisea* LS were determined using the thermostated stopped-flow instrument at 25°C. The left syringe contained 200 mM Tris–HCl, pH 7.5, and varying concentrations of DMRL (0.0675 to 2.0 μM). The right syringe contained 0.4 μM *M. grisea* LS in 200 mM Tris–HCl, pH 7.5. The reactions were monitored by following the quenching of DMRL fluorescence upon binding to the enzyme (nearly complete quenching when bound). Excitation was at 390 nm and emission was through a 450-nm-long pass filter.

RESULTS AND DISCUSSION

Isomerization about a C=N double bond can occur via either an in-plane inversion at the nitrogen center or an out-of-plane rotation about the double bond. The in-plane inversion does not require the double bond to be broken, while the out-of-plane rotation does. Therefore, the former pathway is expected to be preferred. Both semiempirical and high level ab initio molecular orbital methods are capable of providing an estimations of the inversion barrier. Since the compounds involved (**3** and **4**) are rather large, high level ab initio molecular orbital method cannot be applied directly. The semiempirical method can be applied to a very large system as in this case; however, these methods may not be accurate enough to give a definitive answer. Therefore, we decided to calibrate the semiempirical AM1 method on a model compound where a high level ab initio molecular orbital method can be applied. The comparison between the AM1 and high level ab initio results provides us with information about the uncertainty in the AM1 result. First of all, we carried out both AM1 and G2 calculations on compound **6** (Fig. 2).

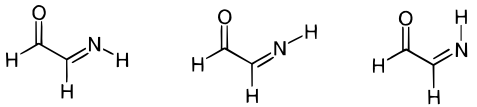

FIG. 2. Model compounds used for the calculation of energy barriers at the G2 level.

The G2-calculated forward (*trans* → TS) and backward (*cis* → TS) barriers for **6** are 25.5 and 28.5 kcal/mol, respectively. The corresponding AM1 values are 19.4 and 23.9 kcal/mol, respectively. The higher barrier for isomerization from the *cis* isomer is due to a favorable electrostatic interaction present in the *cis* isomer. The G2 results are generally very accurate; if we take these values as the reference, the AM1 barrier is in error by five to six kcal/mol. After thus establishing the reliability of the AM1 result, the inversion barrier for the intermediate in the LS-catalyzed reaction (the isomerization of **3** to **4**) was investigated using the AM1 method. In the calculations, the irrelevant ribityl group was replaced by a methyl group. The calculated AM1 barrier is 15 kcal/mol. In view of the performance of AM1 on the model system, the barrier should be corrected by about 4.6–6 kcal/mol. After this correction, the isomerization barrier is in the range of 19.6–21 kcal/mol. The calculated barrier heights are in line with experimental values for imines and other related compounds (24). One may argue that the estimated barrier is only for gas phase isomerization and the inversion barrier in the active site of LS may be different. However, the difference is expected to be small since the isomerization does not involve ionic species and no direct interaction between the imine moiety of the intermediate and protein is present as indicated by the crystal structures (in the docked complex).

Kinetic parameters obtained at 25°C for the *E. coli*, *M. grisea*, and spinach lumazine synthases are listed in Table 1. In the steady state, the *M. grisea* LS is a superior catalyst in comparison to the other two enzymes. The single-turnover rate for *M. grisea* LS is about 140-fold greater than its steady-state rate (k_{cat}). The single-turnover rates for the *E. coli* and spinach enzymes were not determined because there were significant lags in the pre-steady state traces that monitored the production of DMRL (Fig. 3A), unlike the simple exponentials seen for the *M. grisea* LS (Fig. 3B). On the basis of the steady-state k_{cat} values, free energies are estimated as 19.7 ± 0.1, 19.2 ± 0.1, and 19.7 ± 0.1 kcal/mol for the respective enzymes (Table 2). The single-turnover rate for the *M. grisea* LS provides a significantly lower barrier.

TABLE 1

Kinetic Parameters Determined at 25°C and pH 7.5 for the LS Enzymes Characterized

Parameter	*E. coli*	*M. grisea*	Spinach
k_{cat} (s^{-1})	0.024 ± 0.0007	0.052 ± 0.001	0.023 ± 0.0004
K_m(ARAPD) (μM)	10 ± 1	2.8 ± 0.4	21 ± 2
K_m(DHBP) (μM)	21 ± 5	0.92 ± 0.3	26 ± 3
Single turnover (s^{-1})	ND[a]	7.2 ± 0.1	ND[a]

[a] ND, not determined.

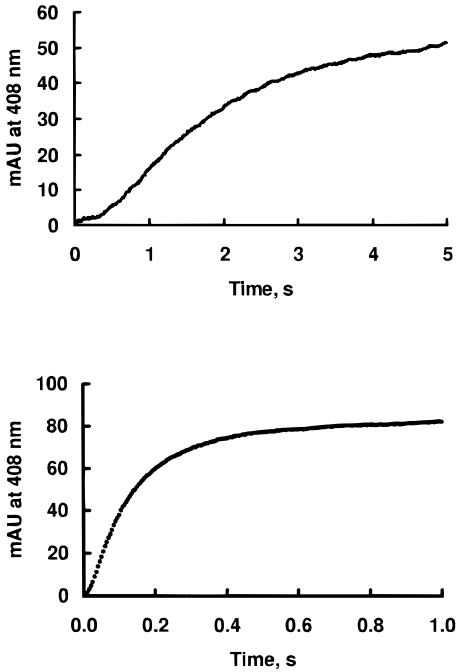

FIG. 3. Pre-steady state traces for the *E. coli* LS (upper panel) and the *M. grisea* LS (lower panel). The single-turnover reactions were monitored for absorbency changes at 408 nm to detect product DMRL.

Steady state rates of catalysis were determined for the three enzymes between 24 and 40°C (Fig. 4A). Pre-steady state rates for the *M. grisea* LS were determined within this range of temperatures (Fig. 4B). Lower temperatures were avoided because the large *E. coli* and spinach enzymes dissociate and lose catalytic activity at lower temperatures (D. Jordan and P. Viitanen, unreported results). Activation energies and the associated thermodynamic parameters are listed in Table 2. As might be anticipated, the enthalpic term for the steady-state and pre-steady state measurements dominates; the entropic term is small and in some cases within the error of the measurement.

The 140-fold more rapid rate determined for the *M. grisea* LS in the pre-steady state over the steady state indicates that an event subsequent to DMRL formation on the

TABLE 2

Thermodynamic Parameters (kcal/mol) at 25°C and pH 7.5 Calculated from the Steady-State and Pre-Steady State Rates for the LS Enzymes Characterized

Parameter	*E. coli*[a]	*M. grisea*[a]	*M. grisea*[b]	Spinach[a]
ΔG	19.7 ± 0.1	19.2 ± 0.1	16.3 ± 0.2	19.7 ± 0.1
Ea	21.0 ± 1.0	21.5 ± 0.7	11.0 ± 0.3	20.8 ± 0.4
ΔH	20.4 ± 1.0	19.9 ± 0.7	10.6 ± 0.3	20.2 ± 0.4
−TΔS	−0.7 ± 1.0	−0.7 ± 0.7	−5.7 ± 0.3	−0.5 ± 0.4

[a] Steady State k_{cat} rates.
[b] Pre-steady state single-turnover rate.

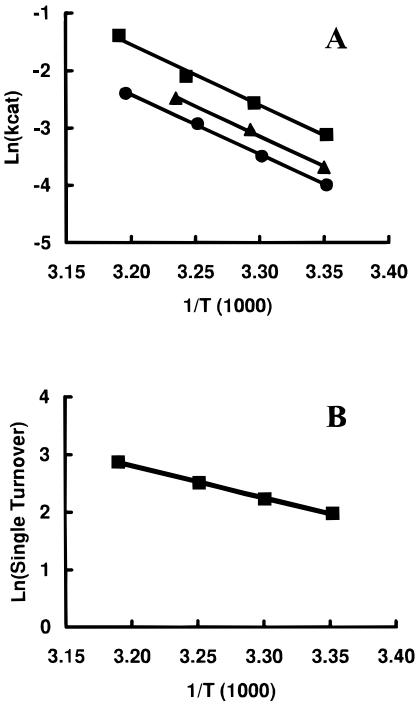

FIG. 4. Arrhenius plots for the rates catalyzed by LS. Natural logs of the steady state (A) and the pre-steady state (B) rates (rates in s^{-1} units) for the LS enzymes are plotted versus the inverse of the temperature in degrees Kelvin times 1000. (▲) *E. coli* LS. (■) *M. grisea* LS. (●) Spinach LS.

enzyme is largely rate determining to the steady-state rate. For example, one or more of the products may have a slow off rate. A lower boundary for the off rate of product phosphate was estimated as about 1 ± 0.1 s^{-1} for the *M. grisea* LS from the burst experiments using an orthophosphate detecting system (instead of monitoring DMRL) at pH 7.5 and 25°C; in the same experimental session, the rate of DMRL formation was estimated as 6.2 s^{-1}. At pH 7.5 and 25°C, the off rate for DMRL from the *M. grisea* LS was determined as 0.37 ± 0.04 s^{-1}, a value that is seven-fold larger than that of k_{cat} (Fig. 5). The experiment determined the association rate (1.4 s^{-1} μM^{-1}), the dissociation constant (0.26 μM) for DMRL from the enzyme, and a stoichiometry of approximately one to one for DMRL to the enzyme protomer. Clearly, there must be another slow step on the order of 0.1 s^{-1} following product formation (e.g., an isomerization step) that more fully accounts for the low value for k_{cat}.

We studied the pH dependencies of the *M. grisea* LS pre-steady state rate of DMRL formation and determined pK_a and pK_b values of 5.8 ± 0.05 and 8.9 ± 0.04, respectively (Fig. 6). It has been proposed (7) that the ND1 atom of His127 of *M. grisea* LS (His88, *B. subtilis* numbering) serves to abstract a proton from the methylene in the transformation of **1** to **2,** plausibly accounting for the determined pK_a of 5.8. The reason for the drop in activity on the basic side may be due to slowing the rate of dehydration

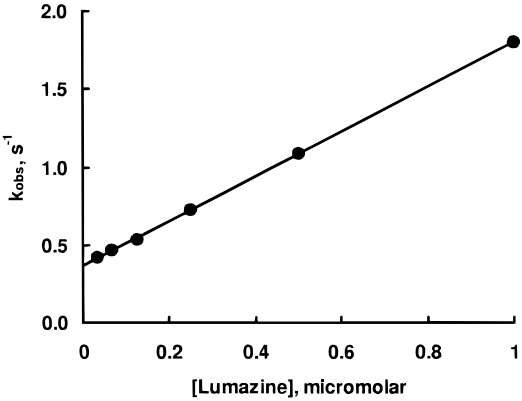

FIG. 5. Association and dissociation rates of DMRL from *M. grisea* LS. The curve is fitted to a line.

of a carbonolamine intermediate in the formation of **1** (from the initial addition complex of DHBP and RAADP) or slowing the rate of dehydration of the carbonolamine **5** to yield **6.** That is, either carbonolamine may have a pK_a approximating this pH (8.9) on the enzyme and either may impose a rate limitation. From the single proton in the fitting on the basic side it can be interpreted that only one of the carbonolamine dehydrations imparts a significant rate limitation in pre-steady state.

CONCLUSIONS

LS is expected to have little influence on the rate of the isomerization of **3** to **4** (Fig. 1), and the isomerization step imposes a significant barrier to the rate of catalysis by LS. This contrasts with the direct roles of active-site, amino acid side chains in mediating the other partial reactions. First, the active site residues have several contacts with the substrates DHBP and RAADP positioning them for forming the intermediate **1.** Additionally, there is a role for an active-site base, His127 (*M. grisea* numbering), in converting **1** to **2.** The steady-state k_{cat} of the *M. grisea* LS is significantly

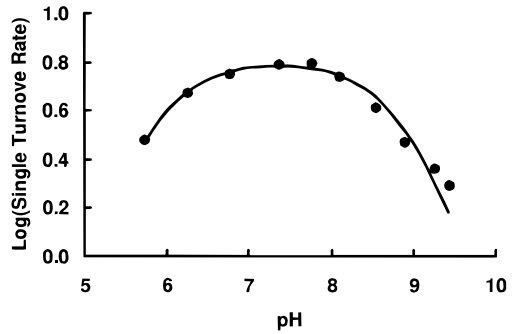

FIG. 6. pH profile for the formation of DMRL by *M. grisea* LS in the pre-steady state. Rates are in units of s^{-1}. The curve is fitted to the data using Eq. [2].

limited by the release of product DMRL. The more simple quaternary structure of the *M. grisea* LS allowed for pre-steady state determinations that could not be obtained with the bacterial and plant enzymes examined in this work. The larger 60-mer icosahedral, capsid-like LS enzymes from *E. coli* and spinach appear to have significant rate limitations imparted by the rates of substrate association as suggested by the independent experimental results of this work and elsewhere (*13*).

REFERENCES

1. Bacher, A. (1991) *in* Chemistry and Biochemistry of Flavoproteins (Müller, F., Ed) Vol. 1, pp. 215–259, CRC Press, Boca Raton, FL.
2. Volk, R., and Bacher, A. (1988) *J. Am. Chem. Soc.* **110,** 3651–3653.
3. Kis, K., Volk, R., and Bacher, A. (1995) *Biochemistry* **34,** 2883–2892.
4. Bacher, A., Baur, R., Eggers, U., Harders, H., Otto, M. K., and Schnepple, H. (1980) *J. Biol. Chem.* **255,** 632–637.
5. Bacher, A., Ludwig, H. C., Schnepple, H., and Ben-Shaul, Y. (1986) *J. Mol. Biol.* **187,** 75–86.
6. Ladenstein, R., Shneider, M., Huber, R., Bartunik, H. D., Wilson, K., Schott, M., and Bacher, A. (1988) *J. Mol. Biol.* **203,** 1045–1070.
7. Ritsert, K., Huber, R., Turk, D., Ladenstein, R., Schmidt-Base, K., and Bacher, A. (1995) *J. Mol. Biol.* **253,** 151–167.
8. Mörtl, S., Fischer, M., Richter, G., Tack, J., Weinkauf, S., and Bather, A. (1996) *J. Biol. Chem.* **271,** 33201–33207.
9. Goldbaum, F. A., Polikarpov, I., Cauerhff, A. A., Velikovsky, C. A., Braden, B. C., and Poljak, R. J. (1998) *J. Struct. Biol.* **123,** 175–178.
10. Jordan, D. B., Bacot, K. O., Carlson, T. J., Kessel, M., and Viitanen, P. V. (1999) *J. Biol. Chem.* **274,** 22114–22121.
11. Persson, K., Schneider, G., Jordan, D. B., Viitanen, P. V., and Sandalova, T. (1999) *Protein Sci.* **8,** 2355–2365.
12. Garcia-Ramirez, J. J., Santos, M. A., and Revuelta, J. L. (1995) *J. Biol. Chem.* **270,** 23801–23807.
13. Kis, K., and Bacher, A. (1995) *J. Biol. Chem.* **270,** 16788–16795.
14. Cushman, M., Mavandadi, F., Kugelbrey, K., and Bacher, A. (1997) *J. Org. Chem.* **62,** 8944–8947.
15. Cushman, M., Mavandadi, F., Kugelbrey, K., and Bacher, A. (1998) *Bioorg. Med. Chem.* **6,** 409–415.
16. Cushman, M., Mihalic, J. T., Kis, K., and Bacher, A. (1999) *Bioorg. Med. Chem. Lett* **9,** 39–42.
17. Douglas, J. E., Rabinovitch, B. S., and Looney, F. S. (1955) *J. Chem. Phys.* **23,** 315.
18. Plaut, G. W. E., and Harvey, R. A. (1971) *Methods Enzymol.* **18,** 515–538.
19. Frisch, M. J., Trucks, G. W., Schelegel, H. B., Gill, P. M. W., Johnson, B. G., Robb, M. A., Cheeseman, J. R., Keith, T., Petersson, G. A., Montgomery, J. A., Raghavachari, K., Al-Laham, M. A., Zakrzewski, V. G., Ortiz, J. V., Foresman, J. B., Cioslowski, J., Stefanov, B. B., Nanayakkara, A., Challacombe, M., Peng, C. Y., Ayala, P. Y., Chen, W., Wong, M. W., Andres, J. L., Replogle, E. S., Gomperts, R., Martin, R. L., Fox, D. J., Binkley, J. S., Defrees, D. J., Baker, J., Stewart, J. P., Head-Gordon, M., Gonzalez, C., and Pople, J. A. (1995) Gaussian 94, Gaussian, Pittsburgh, PA.
20. Curtis, L. A., Carpenter, J. E., Raghavachari, K., and Pople, J. A. (1992) *J. Chem. Phys.* **96,** 9030.
21. Curtis, L. A., Jones, C., Trucks, G. W., Raghavachari, K., and Pople, J. A. (1990) *J. Chem. Phys.* **93,** 2537.
22. Dewar, M. J. S., Zoebisch, E. G., Healy, E. F., and Stewart, J. J. P. (1985) *J. Am. Chem. Soc.* **107,** 3902.
23. Webb, M. R. (1992) *Proc. Natl. Acad. Sci. USA* **89,** 4884–4887.
24. Eliel, E. L., Wilen, S. H., and Mander, L. N. (1994) *in* Stereochemistry of Organic Compounds, p. 550, Wiley, New York, New York.